IMECE2016-65718

ADAPTIVE GIMBAL CONTROL APPROACH TO ACCOUNT FOR POWER CONSUMPTION AND LANDMARK TRACKING QUALITY

Akin Tatoglu
Mechanical Engineering
University of Hartford
West Hartford, CT 06117 , USA
tatoglu@hartford.edu

Claudio Campana
Mechanical Engineering
University of Hartford
West Hartford, CT 06117 , USA
campana@hartford.edu

ABSTRACT

Unmanned Aerial Vehicles (UAV) are commonly used for robotics research and industrial purposes. Most of the autonomous applications use visual sensors and inertial measurement units for localization. Design constraints of such systems are defined considering smooth operation requirements such as indoor environments without external forces where input tracking signal is constant during an operation. In this research paper, we simultaneously investigate and compare stability, power consumption and landmark tracking quality of a visual sensor mounted gimbal specifically for rapid UAV motion requirements where input signal continuously varies such as at obstacle rich environments. We not only attempt to find efficient control parameters but also compare these settings with power consumption and landmark tracking quality metric which are vital for mobile robots and localization algorithms. Efficiency of the system response is analyzed with rise and settling time as well as oscillation amplitude and frequencies. These parameters are tested and benchmarked with various voltage and current limitations. In addition to that, different response behaviors were investigated considering landmark tracking quality metrics including feature detection and image blur. We have shown that gimbal stabilization controller under continuously varying input signal requires less responsive behavior to keep landmark tracking accuracy stable. Initial simulation results, system development and experimental setup procedure are explained and behavior plots for each topic are listed and analyzed.

INTRODUCTION

Unmanned Aerial Vehicles (UAV) use vision systems for localization purposes. During rapid maneuvers, it is efficient to keep the camera view angle fixed and leveled that localization algorithm can result with a more accurate trajectory by reducing the image blur and maximize count of tracked landmarks during
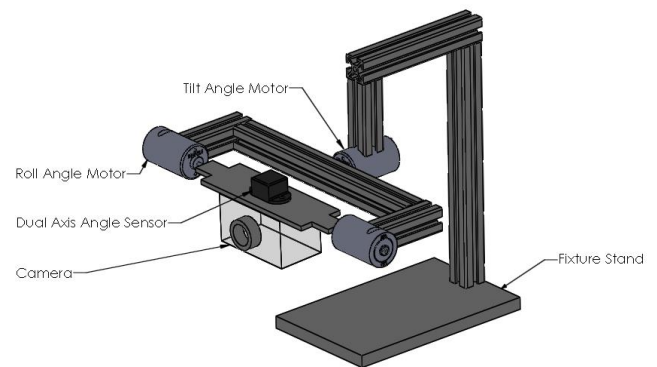

Fig. 1 3D model of the gimbal test setup

inter image process. A practical solution is to use a 3-DOF gimbal. In most cases, it is sufficient to adjust two of the pan, tilt and roll angles which require two actuators and a rig to hold a camera. One of the most important design consideration is the total weight of the gimbal since mobile robots especially aerial ones have limited power sources.

Initial design constraints are determined by physical and computational requirements. One of the solutions to minimize weight is to use as small as possible motor that drives the gimbal. This could be achieved by calculating the minimum torque requirements specific to the UAV. Analyzing vision system characteristics to estimate the maximum velocity and acceleration that could operate without a blur is another design consideration. Both of these solutions improve operation duration since weight is reduced and gimbal battery consumption is minimized by limiting peak current requirement. The challenges to generate a methodology to optimize torque requirements as well as minimize motor weight are to analyze

the control system of such system concurrently with image processing requirements.

In this research paper, we simultaneously investigate stability, power consumption and localization accuracy of a visual sensor mounted gimbal. We not only attempt to find efficient control parameters but also compare these settings with total power consumption and landmark tracking quality. Efficiency of the system response is analyzed with rise time, settling time and overshoots. Moreover, these parameters are tested and benchmarked with various voltage and current limitations. Even if one setting has a lower rise time (rapid angular motion), it might cause a blur or less intersecting interframe area that visual localization quality might get reduced. To consider all of the above items, each solution is studied individually and then analyzed concurrently which is discussed in the following sections.

Previous Work

In common, stabilization system of a gimbal with mounted visual sensors uses a motor to drive each axis and utilizes inertial measurement sensors to supply feedback signal of yaw, pitch and roll angles. One of the many research efforts [1] studies development of a sensor system consisting of a camera with an Infrared sensor (IR) sensor as well as an integrated navigation system. All components are assembled on a gimbal.

The gimbal is controlled with a motor on each axis and system is stabilized with gyros: two outer joints and two inner joints. The outer joint has no mechanical constraints and can rotate continuous 360 degrees, but the inner joint is constrained. Digital encoders measure the pan and tilt angles and an optical angle sensor measures the angles of the inner gimbal. The navigation system estimates the position of camera and orientation of its optical axes (local frame). An electronic speed system (ESC) is used to drive gimbal actuators and control the tracking of reference signal. The goal is to respond quickly while not exceeding operational range of the inner gimbal damping mechanism. Inner damping blocks effects of high frequency rotational vibrations to cameras, which might cause blur of the images. A drawback that comes with this solution is that large accelerations or decelerations excite the flexibility, which will cause the inner camera gimbal to oscillate.

Another research project aims to generate panoramic images as an alternate to stabilized camera single view image sequences for localization [2]. This method generates more occluding inter frame area that localization is executed with higher accuracy. Specifically in the way these new technologies have allowed camera and sensor gimbals to be place in smaller platforms, like "miniature" UAV systems. The prototype consisted of a 3 axis mechanism driven by DC motors with incremental encoder feedback and an AHRS unit for angular movement corrections. The goal is for the gimbal to take 360 panoramic images without the need of mechanically repositioning the camera, but with rotation of the overall sensor frame.

The report [3] shows us the design of a controller for an inertial stabilization system of two degrees of freedom with two induvial control of inner and outer local frames. While one of them keeps the body aligned, the other one applies inverse dynamic equation to predict the next required motion to stabilize the line of sight with a digitally stabilized camera.

Another approach is to fuse a light detecting and ranging (Lidar) system generated point cloud with a GPS signal and Inertial Measurement Unit (IMU) [4]. Authors developed a low-cost UAV with a Lidar on board to provide spatial resolution datasets. Since main goal of the research is to develop a mapping system, it generates a high density point cloud with 62 data points per meter square.

Similar visual localization solution could be solved with a more advanced equipment such as Digital Elevation Map (DEM) through an IR image sequences and an altimeter [5].

Power consumption of gimbals was studied as well. The research effort [6] demonstrates that the kinematics of a control-moment gyroscopes (CMGs) multi body robotic system can be optimized so that a minimal amount of power is used. Solution uses a quadratic cost function which is the sum of the squares of power for each gimbal system. The gimbals used were controlled such that the body kinematics are optimized for power. The paper also studies "non-recoverable powers" components and found that energy requirement is reduced by up to 42.1% with their control and power optimizations.

Visual Simultaneous Localization and Mapping (SLAM) is the most common localization method that utilizes location uncertainty of surroundings to determine position of a robot or a vehicle itself [7]. While the robot is traversing, failure of localization or reconstruction is often caused by severe motion blur. The research team proposed a visual SLAM algorithm combined with image deblurring. Many recent visual SLAM systems ensure a frame rate of at least 10 Hz for the real-time performance. The exposure time does not exceed the frame interval, and within this short exposure time the movement of a pixel can be approximated as a straight line. By this assumption, the team parameterized the blur kernel.

Another research effort [8] created a visual tracking device for artificial landmarks based on color histograms. Authors divided UAV self-localization into three categories: Geometric, topological and individual landmarks to overcome image processing issues during stochastic localization approach.

Our approach

While a high discharge capable power supply could generate high current and allow the system to generate rapid motion, high velocity might cause blur in the image. On the other hand, lower current –if adjusted correctly— can generate a physical boundary that will automatically reduce peak velocity as well as maximum angular acceleration of the system. If a battery is discharged at a faster rate than recommended, it delivers less capacity in the longer run. In addition to that, peak current consumption is limited naturally; therefore power consumption could be regulated smoothly.

In our approach, a camera rig is assembled with a tilt sensor on each DOF. First, various motion profiles were created to test camera responses. For each motion type, the amount of blur occurred was benchmarked to analyze sensor response. These values –velocity and acceleration— are used to limit the overall system. The system is tested with various P and PI parameters –

initially with simulations followed by experiments. For each control structure, minimum voltage and current requirements are calculated to drive the system from initial state to leveled state (pendulum like motion). Output is sampled at 20Hz and response plots are listed and compared. In addition to that, simulated response plots are included for further design purposes. Finally, all data are analyzed together and a set of items listed for gimbal design constraints.

The next section discusses the system's transfer function and the generated block diagram followed by landmark tracking methodologies and defined quality metrics. The last two sections before the conclusion discuss the experimental setup and compare results.

GIMBAL CONTROLLER DESIGN AND DEVELOPMENT
System Design and Simulation

The transfer function of the system is defined and various inputs were experimented. Commonly known, the electrical motor transfer function is given by

$$G_g = \frac{K}{s((J*s+b)*(L*s+R)+K^2))} \qquad (1)$$

where K is the feed forward gain of closed loop system which represents various P and I controllers. While J is the load, L represents the inductance due to windings and R is the resistance. The parameter b is viscous friction coefficient. Specific values used for simulations are given by J = 3.2284 pounds, b = 3.5077E-6, R = 8 ohms and L = 2.75E-6 Henry. Finally, the actual transfer function used to generate the block diagram is given by

$$G_g = \frac{0.0548}{7.102e-11\,s^3 + 0.0002066\,s^2 + 0.003228\,s} \qquad (2)$$

The unit response of the system is studied with various P and PI values and shown in Fig. 2. While P I controllers generate a zero steady state error, the time required to reach the goal might not be sufficient due to high maneuver of the UAV which results with varying input signal. Therefore, dominant parameter to consider is the rise time. The block diagram is discussed in the following section.
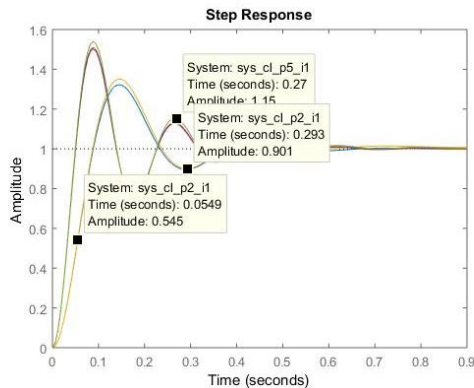

Fig. 2 System response with varying P and I values.

Block Diagram

Controller design, prototyping and implementation are done using LabVIEW block diagram programing software which interfaces to a general purpose input/output (GPIO) data acquisition (daq) card. The main components of the program are executed within the framework of a while loop. The block diagram program for the overall system is shown in Fig. 3 and implementation details are discussed in the next paragraph.
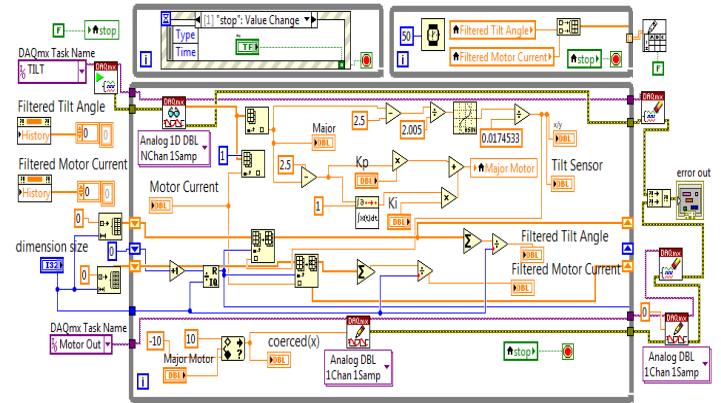

Fig. 3 Block diagram of the overall system

Channel input/output (I/O) assignments are done using the data acquisition card's configuration utility. These assignments are saved as tasks. Two tasks were defined. One task contains the assignment for two analog inputs (one for tilt sensor and one for current sensor) while the second task contains an assignment for one analog output—control signal to motor driver. The analog input channels will read the signals in volts within a range of -10 to +10 Volts. Control signal or analog output is supplied from the card as a variable voltage value in a range between -10 and +10 volts as well.

In channel assignment tasks several channel setting parameters are available for configuration. Among them are the type of data acquisition mode and terminal configuration. For this case the data acquisition mode was set as one sample on demand meaning that one sample of data is acquired for each execution of the while loop in the Labview program. In this manner by timing the while loop, sampling rate can be adjusted. Terminal configuration was set to reference single ended (RSE) meaning the sensor voltage is read relative to a common or single ground.

Once the tasks for the channel assignments are defined they are implemented in LabVIEW using Daqmx sub VI's that access or write to the data acquisition card. In the case of analog inputs, these sub VI blocks are used to declare selected channel tasks and enable data acquisition at the beginning of the program, read data during the execution of the program (while loop), and erase the tasks after the program is stopped. For the analog output the Daqmx sub VI blocks are used to declare the channel task used at the start of the program, write data during the execution of the program and erase the tasks after the program is stopped.

3   Copyright © 2016 by ASME

In addition to the task implementation, numeric control variables are defined and set to the desired values before the start and after the termination of the program or while loop. An example is setting the analog output for the motor to 0 Volts after the program stops or the emergency stop is pressed.

Given the environment in which the sensors operated and the range of measurements, some form of signal conditioning was required to filter out the noise for both the tilt sensor and the current sensor. A method consisting of averaging the sensor data based on select range of samples was used as a means of filtering out the noise. This was implemented in the LabVIEW program by using array and arithmetic block functions to store a range of data (selectable by the user) and calculate the average of the data over a number of samples.

In order to properly display the data acquired from the tilt sensor in angular units a conversion from voltage to degrees is necessary. For the tilt sensor used the conversion equation is defined as

$$\varnothing = \left[\frac{V_{out} - Zero\ Angle\ Voltage}{Sensitivity} \right] \qquad (3)$$

Therefore arithmetic blocks combined to represent this equation are implemented in the LabVIEW program. The implementation of the Proportional Integral Derivative (PID) controller is done by using arithmetic blocks such as multiplication / gain blocks for the individual PID gains and integral and derivative blocks for integral and derivative functions respectively.

The output from the PID controller program section needs to be scaled to a voltage output range supported by the data acquisition card (-10 to +10 Volts) and voltage output required by the motor drive. Hence, to prevent the program from terminating unexpectedly due to voltage signals generated outside of the range supported by the data acquisition card, an in range and coerce block is used prior to writing data to the daq card.

In order to log the data from the test runs that were performed, a parallel while loop was established that would take the acquired data and store it to a database file for each execution of the loop.

Finally several numeric indicator blocks and waveform chart blocks are used in the program to display the data from the tilt and current sensor as well as voltage output to the motor drive. In the case of the tilt and current, data from these sensors are displayed in waveform charts as shown in Fig. 3.

Design Components and Development

This section discusses experimental setup details. Pictures of rig built and visual matrix are shown in Fig. 4. A diagrammatic representation of the system is shown in Fig. 5. The gimbal is a 2 axis system consisting of two DC motors (one for each axis), tilt sensor, current sensor and camera. This system is interfaced to a computer based system used as the processor / controller. It consists of data acquisition software and hardware which is used for programming and controlling the gimbal.
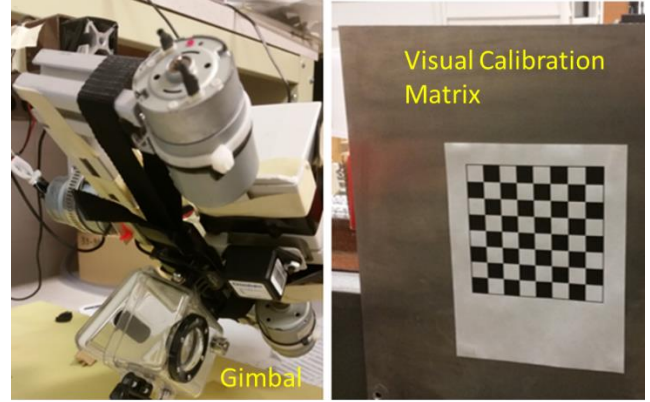

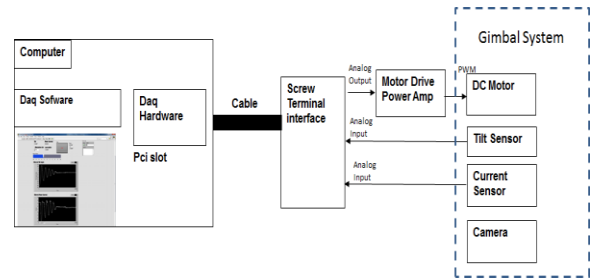Fig. 4 Gimbal, camera and visual calibration template

Fig. 5 Diagram representation of the gimbal test setup

The computer based system is composed of data acquisition software which interfaces to a general purpose input/output card. The card has an input resolution of 12 bits and has 16 channels of analog input, 2 analog output channels, 8 digital channels configurable as input or output, two 24-bit counters and maximum sampling rate of 200 kS/s. For test setup, this card is used to acquire the signals from the tilt and current sensors as single ended analog inputs and generate signals to the motor driver as analog output. Hence two analog input channels and one analog output channel were configured.

For actuation of the system, brush type DC motors were used. These motors have an operating range between 9.6 to 30 Volts with a 24 Volt nominal operational voltage. It is capable of outputting approximately between 3 to 60 watts. One motor is installed per each axis of motion.

The driver outputs a Pulse Width Modulated (PWM) voltage to the motors. The minimum operating voltage for this equipment is 24 Volts and it is capable of handling a current of 6 Amps continuous and 12 Amps peak. Measurement of angular position for the two axes is done using a dual axis tilt sensor. It is an accelerometer based sensor with signal conditioning to output analog voltage representing angular displacement data. This sensor is capable of reading angles of rotation from two perpendicular axis of rotation. It has a ± 75 degree range of operation with a sensitivity of 35mv/degree and a resolution of 0.03 degrees. With excitation voltage supplied, the sensor will output the angular displacement in volts in a range between 0 and 5 volts where 2.5 volts represents level reference or 0 degrees.

Measurement of current is done utilizing a resistance based sensor placed on the negative side (return) between the motor

driver and the dc motor. This sensor is capable of measuring current up to 2 Watts of power. Measurement across this sensor outputs an analog voltage. The relationship between the measured voltage and current is such that 1mv is equal to 1mA. The electrical schematic and placement within the system is shown in Fig. 6.
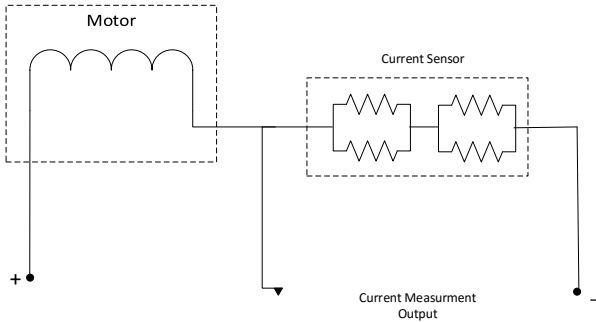

Fig. 6 Electrical schematic of the current sensor

With the system at 45 degrees angle the gimbal is tested for different values of proportional gain. The system response is recorded as the gimbal goes from -45 degrees to 0 degrees which is the target level position. Both the tilt angle and the current is recorded vs. time. An example of a test run is shown in Fig. 7.
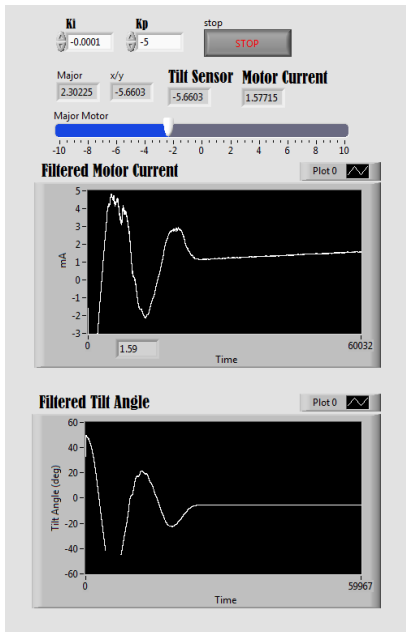

Fig. 7 Test run results for tilt angle and motor current

LANDMARK TRACKING

Continuously detected landmark positions are not only used to generate a map but also are used to localize robots such as an UAV. The accuracy of landmark position has a direct effect on the position accuracy. Fig. 8 shows a generic scheme of the definitions with a landmark.
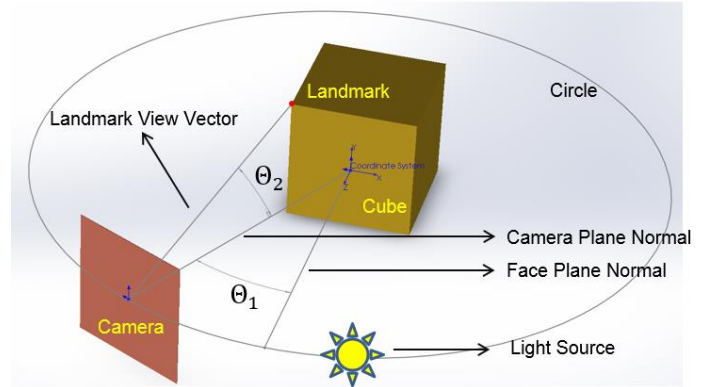

Fig. 8 Landmark Properties and Definitions

In the above figure a cube is used to represent the real world environment and a geometrical relationship between camera plane and a landmark is defined. The camera mounted on the gimbal has its own local frame. The cube's local coordinate system is shown in blue in the figure. In the current perspective, the distance from the camera plane to the center of the cube is equal to the radius(r) of the circle. Θ_1 defines the angle between cube's surface normal and camera plane normal. The landmark's location is marked in red. Θ_2 defines the view angle.

During the motion of the gimbal, Θ_1 and Θ_2 will vary. However, the same real world object is required to be identified as a landmark and associated continuously. If the landmark has a signature defining its attribute(s), it could be exhaustively sought in the scene. If the camera motion could be predicted, the new location of the landmark in the camera plane could be estimated. In this case, an algorithm could define the limited search area to identify the landmark. Signature of a landmark is its numeric descriptor calculated by the feature detection algorithm.

A landmark could be a corner, an edge, a line or a custom shape. It should be noted that robot has no priori information about map or environment properties to execute a localization algorithm. Therefore, it should be capable to identify real world attributes and more importantly it should be capable of continuously identifying landmark's signature on generated map to localize itself such as in SLAM problem. The landmarks may be identified based on the following attributes.

a) Distance: Resolution of the scene is limited with quantity of light sensors in a camera. Near objects will be observed with richer information. A real world attribute might not be able to be identified if the distance is high.

b) Angle: While landmark view vector and camera normal angle is getting narrower, the area that could be observed is proportionally reduced with the sinus of the angle.

c) Ambient Light Variation: Even if there is a fixed point light source in the environment, these changes might also lead different amount of ambient light reflection from the observed surface.

Any rapid change of the above parameters or high noise –such as a blur— reduces the quality of tracking which is discussed in the next subsection.

Landmark Tracking Quality Metrics

Landmark tracking quality metric defines the ratio of count of landmarks marked versus all image size and is used to analyze the effect of different motion types as well as lighting in continuous image sequence. For a fair evaluation, the algorithm is supposed to be tested on the same texture (Fig. 4, right image). However, during motion the scene varies. To overcome this issue, texture location is manually calculated and homography matrix; which contains 3D plane transformation and rotation information; is manually calculated from known positions and for each step, texture area is extracted from the scene. Fig. 9 shows texture area in the scene.
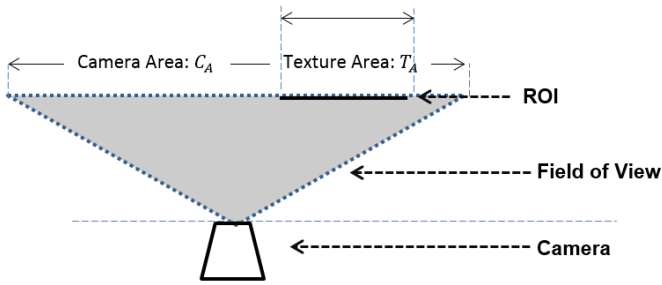

Fig. 9 Extraction of Texture Area with homography Transformation

After transformation is calculated, the same texture will be used as a region of interest that all algorithms will be using as the same input area. Finally for each step, landmark observability is determined by the ratio of marked landmarks per texture which is given by:

$$L_O = \frac{N_D}{T_A} \qquad (4)$$

Fig. 10 shows the plots of landmark tracking quality, L_O, for pan angle. In this experiment view angles Θ_2 varies between -23° to 23°. All L_O values around 0° decrease. It should be noted that this point is where Θ_1 is 0°. Other than that all values are stable with varying panning angle. Significant result is that Features from Accelerated Segment Test (FAST) method is more stable for various different angles and distances that it could track a landmark during panning well.

EXPERIMENTAL DESIGN

Experimental Setup

A two degrees of freedom camera gimbal using aluminum rectangular rods and a small camera holder was constructed for the experimental setup. A feedback software code was developed using a tilt sensor which was placed at the bottom of the plate where the camera holder was placed. The software consisted of a simple feedback loop and a k_p controller, the value for this control gain was found by trial and error.

For this research the experimental setup described was used to test the reactions of the main DC motor in only one axis. The secondary motor that interacts directly to the camera plate and works the up and down motion of the camera was disabled and made stationary. Then the gimbal was set on a stand that would
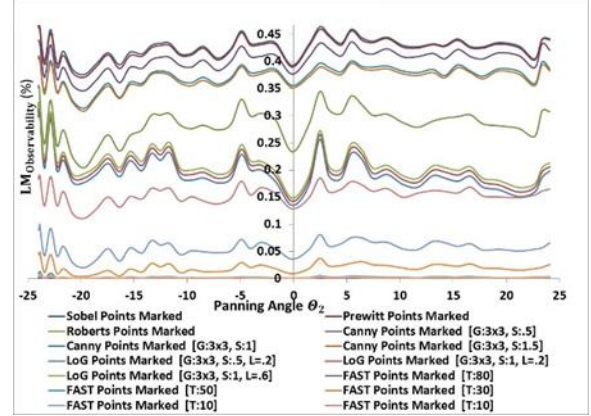

Fig. 10 Landmark Quality vs Panning Angle with various landmark detection techniques

hold the whole system in the air and allow freedom of uninterrupted movement for the axis of interest.

The tilt sensor work by giving out two analog voltages. One for each axis of movement, and it works with a 2.5V reference level when the tilt sensor is flat, or with no rotation. Using this analog input the control software worked but we needed to know the exact degree, so we used the formula provided by the maker where the sensitivity of the sensor is 35 (mV/deg) which is given by Eq. 3.

The first test performed was a base one, to see if the requirements were met and how the motor interacts with a certain torque being applied and specifically to know the voltage required by the motor to move the gimbal. To do this gimbal was let fall to about 75 degrees from the horizontal axis. The next step was to develop a more visual control software using LabVIEW. In this software we would be able to see exactly how much voltage was being used by the motor and we plotted the rotation of the gimbal, creating the software with a reference input of 0 degrees from the tilt sensor. Then as soon as the control system is run, feeding the motor voltage is started, and it is slowly increased until we see the motor moving the gimbal.

The next step was to execute the same experiment with different k_p values varying from 3 to 10 with increments of 0.5. Voltage required to start the motion is detected and the angle at which it is settled with that certain k_p and voltage is logged.

Current Measurement

After executing this experiment, it is decided that to analyze the power consumption of the system in more detail, it will be helpful to plot current consumed by the motor with respect to angular position during complete motion till the system is stabilized –tracking error is minimized. Power input is kept at 24V throughout the rest of the experiment and current consumption is logged. A circuit with a common ground with the

motor that translates that voltage to amperage through a bridge circuit using 1 ohm resistors was implemented.

EXPERIMENTAL RESULTS
Angular Response with P and PI controller

Initial experiments were applied with only proportional controller components. Fig. 11 shows the measured response plots of values $k_p = 2, 8, 10$ and 14. As expected, there is a steady state position error. k_p=14 has the minimum steady state error, while k_p=2 has the minimum oscillation.

Same experiment is applied with PI controller, $k_p + \frac{k_I}{s}$. Since k_p=10 has a reasonable response, three different k_I values were experimented and plots are shown in Fig. 12. For comparison, k_I=0.001, k_p= 5 is also shown in the same plot. While integrator guarantees that poles are on the left half plane of the imaginary axis, steady state errors are zero for all values. PI settings of k_I=0.01, k_p= 10 resulted with shortest transient response duration while rise time is similar to other responses. Minimum oscillation is observed with lowest proportional gain, k_p= 5.
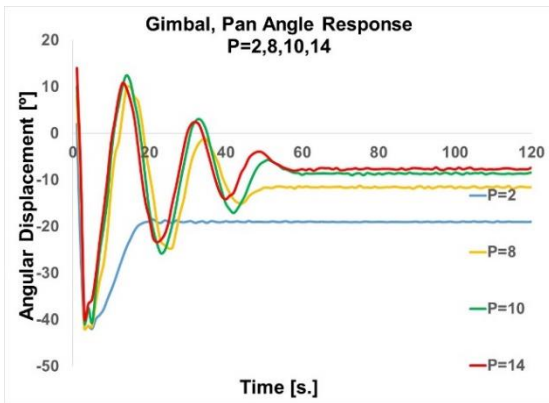
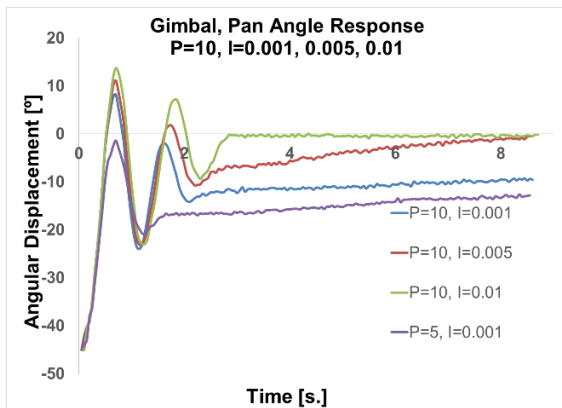Fig. 11 Pan angle response measurement with varying k_p values

Fig. 12 Pan angle response measurement with k_p =10 and varying k_i values

Energy Consumption

Energy consumption is calculated in watt-second. Same PI controllers of the previous plot are used to present power

consumption and shown in Fig. 13. With k_p values of 10, there is a small amount of oscillation, but most of them behaves linear once response reaches to steady state. It should be noted that while setting k_p=10, k_I=0.005 didn't result with the best response (min. error), it consumes most power. Also, k_p=5, k_I=0.001 setting consumes 11% less power than the best response setting at Fig. 12 which is k_p=10, k_I=0.01.
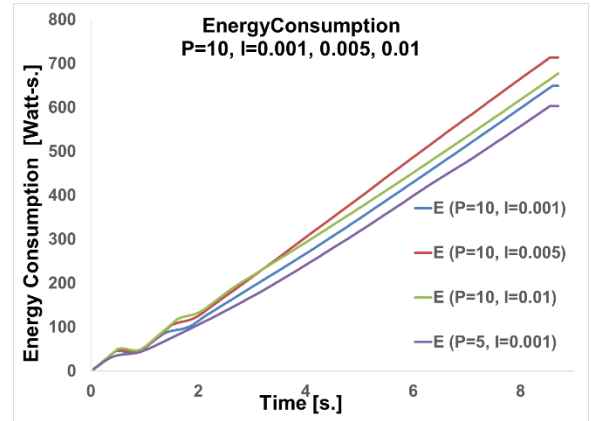
Fig. 13 Energy consumption of various controllers

Landmark Tracking Quality

FAST corner detect algorithm is applied as described in Section-III. In addition to that, blur metric is calculated for each frame and both values are normalized. Then final Landmark Quality Metric (LQM) is given by

$$LQM = 0.5 \ L_o + 0.5 \ BM \qquad (5)$$

where BM is blur metric and same weight is applied to both components. Results are shown in Fig. 14. It is observed that oscillatory motion of gimbal causes Θ_1 and Θ_2 angles (discussed in Section-III) vary in a way that LQM behavior generates peak points for each local extremum of the angular displacement plot shown in Fig. 12.
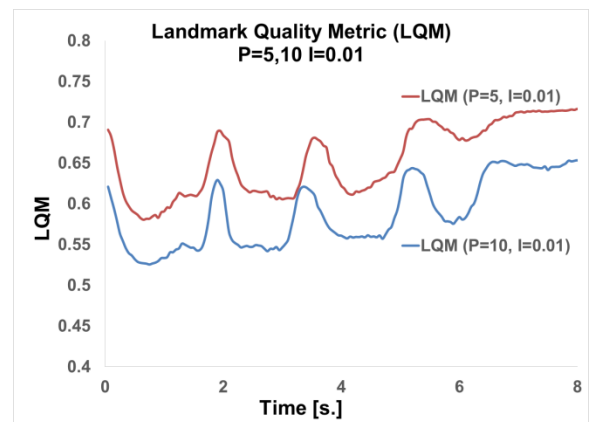
Fig. 14 Landmark Quality Metric comparison for P and PI settings

Overall Analysis

Visual localization of an UAV requires aligning gimbal for a smooth tracking process. When an aggressive maneuver is required, UAV body might experience rapid linear and angular displacement. This action might cause higher failure rate of landmark registration in successive images. In addition to that, if UAV is expected to maneuver rapidly –i.e. windy air, aiming camera on a region of interest— that gimbal controller might not have enough time to reach to steady state since input tracking signal varies rapidly as well. Also, it will keep consuming power to adjust the system while never reaching to a steady state for this short time period before a new input signal is assigned.

When we look at the Fig. 12, it is clear that PI controller has a smaller steady state error with respect to tracking error. However, in best case, it takes more than 3 seconds to reach that goal. In this first three seconds, oscillation of gimbal will not die-out. Moreover, if input signal is continuously changed, this behavior during rise time will be repeated over time. If we look at the P only controller, response of both systems in the first second are similar. From Fig. 11 and 12 it could be concluded that for different variables there won't be much difference if input signal is varying in every 1 second.

Another important point to investigate is power consumption. It is discussed in the previous paragraphs that, advantage of a PI controller starts after 3 seconds and consumes 11% more power. Again, if input signal varies continuously, system will drain power without a benefit of reaching the zero or constant position error goal.

Localization is key point for any type of robotics mission. When Fig. 14 is analyzed, it is observed that slower response results with a smoother landmark tracking process.

Briefly, short rise time is only advantageous if input signal is stable for longer periods of time –i.e. UAV operating with less external effects and following a smooth path. If this is not the case, higher response time will cause more oscillation, more power consumption and less localization accuracy while never reaching the goal. While both solutions have their own trade-offs, it is up to the operator to decide in between. Another suitable solution is to adaptively changing PI settings by analyzing stability of input signal.

CONCLUSIONS AND FUTURE WORK

We have studied gimbal controller response stability while considering power consumption and landmark tracking quality. Multiple experiments with varying P and PI values were executed and plots of controller responses, energy consumption and tracking quality are listed. It is shown that for a smooth UAV operation when input signal is consistent, PI controller is advantageous since it has a shorter rise time and smaller steady state error. However, if input signal changes continuously at every couple seconds while UAV maneuvers rapidly, there won't be sufficient amount of time to reach the zero error goal. In that case, PI solution will keep oscillating and consume more power with higher overall error. Also, it never reaches to steady state while reducing the landmark tracking quality that will result with less localization accuracy. To take advantage of both settings, it

is a suitable approach to adaptively set PI parameters during the mission by analyzing input signal behavior.

In next steps of our research, we will investigate similar situations with real world environments such as windy weather conditions and experiments will be executed for longer periods of time and distances.

REFERENCES

[1] Skoglar, P., 2002, "Modelling and control of IR/EO-gimbal for UAV surveillance applications." Institutionen för Systemteknik

[2] Tiimus, K., and Tamre, M., 2010, "Camera gimbal control system for unmanned platforms," Danube Adria Assoc. Autom. Manuf. 7th Int. DAAAM Balt. Conf. "Industrial Eng., (April), pp. 202–207.

[3] Sangveraphunsiri, V., and Malithong, K., 2010, "Control of Inertial Stabilization Systems Using Robust Inverse Dynamics Control and Sliding Mode Control," 6th Int. Conf. Automot. Eng., (March), pp. 1–10.

[4] Wallace, L., Lucieer, A., Watson, C., and Turner, D., 2012, "Development of a UAV-LiDAR system with application to forest inventory," Remote Sens., 4(6), pp. 1519–1543.

[5] Woo, J., Son, K., Li, T., Kim, G., and Kweon, I. S., 2007, "Vision-based UAV Navigation in Mountain Area," Proc. Conf. Mach. Vis. Appl., May 16-18, 2007, Tokyo, Japan, 1, pp. 3–6.

[6] Carpenter, M., 2008, "Power-Optimal Steering of a Space Robotic System Driven by Control-Moment Gyroscopes," AIAA Guid. Navig. Control Conf. Exhib., (August), pp. 1–15.

[7] Lee, H. S., Kwon, J., and Lee, K. M., 2011, "Simultaneous Localization, Mapping and Deblurring," Proc. IEEE Int. Conf. Comput. Vis., pp. 1203–1210.

[8] Yoon, K.-J., and Kweon, I., 2001, "Artificial Landmark Tracking Based on the Color Histogram," Proc. IEEE Int'l Conf. Intell. Robot. Syst., 4, pp. 1918–1923.